Similarity Analysis for Nonequilibrium Turbulent Boundary Layers*

Luciano Castillo

Xia Wang

Rensselaer Polytechnic Institute, Department of Mechanical, Aerospace and Nuclear Engineering, Troy, NY 12180

In his now classical paper on pressure gradient turbulent boundary layers, Clauser concluded that equilibrium flows were very special flows difficult to achieve experimentally and that few flows were actually in equilibrium [1]. However, using similarity analysis of the Navier–Stokes equations, Castillo and George [2] defined an equilibrium flow as one where the pressure parameter, $\Lambda = [\delta/(\rho U_\infty^2 d\delta/dx)](dP_\infty/dx)$, was a constant. They further showed that most flows were in equilibrium and the exceptions were nonequilibrium flows where $\Lambda \neq$constant. Using the equations of motion and similarity analysis, it will be shown that even nonequilibrium flows, as those over airfoils or with sudden changes on the external pressure gradient, are in equilibrium state, but only locally. Moreover, in the case of airfoils where the external pressure gradient changes from favorable to zero then to adverse, three distinctive regions are identified. Each region is given by a constant value of Λ_θ, and each region remains in equilibrium with Λ_θ =constant, respectively. [DOI: 10.1115/1.1789527]

1 Introduction

Clauser [1] defined an equilibrium boundary layer with pressure gradient (PG) as one where the pressure parameter given as,

$$\beta = -\frac{\delta_*}{\rho u_*^2}\frac{dP_\infty}{dx}, \tag{1}$$

was a constant and the velocity deficit profile normalized with the friction velocity, u_*, was independent of the streamwise direction. Thus, the profiles should collapse into a single curve. However, most flows did not satisfy these conditions, especially flows near separation or separated, where the friction velocity, u_*, was approaching zero. Clauser [1] further concluded that these equilibrium flows were a special type of flows which were difficult to generate and maintain in equilibrium, and therefore most flows were recognized as nonequilibrium flows.

Bradshaw [3] showed that a necessary condition for a turbulent boundary layer to maintain equilibrium was that the contribution of the pressure gradient to the growth of the momentum deficit should be a constant multiple of the contribution from the surface shear stress, which was shown to be the same as Clauser's pressure parameter, β.

Townsend [4] developed a self-preserving theory which was more rigorous than the analysis by Clauser [1]. Unfortunately, Townsend [4] overconstrained the problem by assuming the existence of a single velocity scale. Rotta [5] studied the adverse pressure gradient (APG) flow and showed that the length scale and the velocity scale were given as, $\delta_* U_\infty/u_*$ and u_*, respectively. Obviously, these scalings also failed for flows with strong APG or near separation. Later on, a criterion given as $U_\infty = \alpha(x - x_0)^m$ with $m<0$ was used very often to predict the equilibrium adverse pressure gradient boundary layer by Townsend [6], East and Sawyer [7] and Skåre and Krogstad [8]. However, there have been a lot of disagreements on the range of m in which the equilibrium boundary layer should exist. Kader and Yaglom [9] carried out a similarity analysis on moving-equilibrium turbulent boundary layers with APG. Their so-called moving-equilibrium turbulent boundary layers were restricted to exclude the effects of the upstream conditions, even though many equilibrium flows and near-equilibrium flows fell into this group.

As stated earlier, most of the previous definitions about equilibrium boundary layers were proposed assuming that a single velocity scale existed. However, the classical log-law based on this single velocity scale assumption (i.e., the friction velocity) did not work for all flows, especially for those with strong APG. Furthermore, Coles and Hirst [10] mentioned that the classical scaling laws failed for turbulent boundary layers experiencing strong pressure gradient and for relaxing flow where there was a sudden change in the external pressure gradient or boundary conditions.

Recent results using similarity analysis of the RANS equations by Castillo and George [2] showed that the proper velocity scale for the outer part of the boundary layer was the free stream velocity instead of the friction velocity. Subsequently, an equilibrium boundary layer was found to exist only when the pressure parameter Λ, defined as

$$\Lambda = \frac{\delta}{\rho U_\infty^2 d\delta/dx}\frac{dP_\infty}{dx}, \tag{2}$$

was a constant. Integrating the above equation, a power law relation can be obtained between the boundary layer thickness, δ, and the free stream velocity, U_∞. Furthermore, it was shown that the power coefficient was given by the pressure parameter as $-1/\Lambda$, i.e., $\delta \sim U_\infty^{-1/\Lambda}$. Moreover, if the experimental data after the taken logarithm was plotted, this power law must show a linear relationship if an equilibrium flow existed at all. Surprisingly enough, Castillo and George [2] showed that this was the case for most pressure gradient (PG) flows, and the exceptions were nonequilibrium flows where the pressure parameter was not a constant. In addition, it seemed that only three values of the pressure parameter were needed to characterize all equilibrium boundary layers. One was for the adverse pressure gradient (APG) flow with $\Lambda \cong 0.22$, one for the favorable pressure gradient (FPG) flow with $\Lambda \cong -1.92$, and one for the zero pressure gradient (ZPG) flow with $\Lambda = 0$. This simple definition makes it easier to study the behavior of boundary layers. Most recently, Castillo et al. [11] showed that even flows approaching separation or at separation obeyed this simple relation, and hence remained in equilibrium.

*This paper has been presented in the 32th AIAA Fluid Dynamics Conference and Exhibit June 24–26, 2002, St. Louis, Missouri.

Contributed by the Fluids Engineering Division for publication in the JOURNAL OF FLUIDS ENGINEERING. Manuscript received by the Fluids Engineering Division October 18, 2002; revised manuscript received March 15, 2004. Associate Editor: T. B. Gatski.

There is still another type of flow where $\Lambda\neq$constant, i.e., the "nonequilibrium flow," which needs further investigation. This nonequilibrium flow occurs very often in the case of airfoils where the external pressure gradient usually undergoes from favorable to zero and then to adverse. Another possible case is the relaxed flows as defined by Bradshaw [12], where sudden changes in the external conditions lead to a flow history dependence in the downstream flow. Consequently, they exhibit a very different behavior from those expected in the classical log-law. Therefore, the primary goal of this paper is to study the behavior of nonequilibrium boundary layers using similarity analysis of the equations of motion. In addition, it will be shown that although this type of flow cannot be considered to be in equilibrium since $\log(U_\infty)$ vs $\log(\delta)$ is nonlinear, it is still in equilibrium, but only locally.

2 Similarity Analysis

The outer scales of the turbulent boundary layer must be determined from the equilibrium similarity analysis of the governing equations, and not chosen *a priori*. Castillo and George [2] applied this concept to the outer boundary layer equations in order to determine the mean velocity and Reynolds stresses scales. The present analysis is restricted to a 2D, incompressible turbulent boundary layer, and steady state on the mean. The continuity equation is given as,

$$\frac{\partial U}{\partial x}+\frac{\partial V}{\partial y}=0. \tag{3}$$

The boundary layer equation for the outer flow ($y/\delta>0.1$ typically) reduces to

$$U\frac{\partial U}{\partial x}+V\frac{\partial U}{\partial y}=-\frac{1}{\rho}\frac{dP_\infty}{dx}+\frac{\partial}{\partial y}[-\langle uv\rangle]+\frac{\partial}{\partial x}[\langle v^2\rangle-\langle u^2\rangle], \tag{4}$$

where $U\rightarrow U_\infty$, $\langle uv\rangle\rightarrow 0$ as $y\rightarrow\infty$, $\langle u^2\rangle$ and $\langle v^2\rangle\rightarrow 0$ as $y\rightarrow\infty$ as well according to Tennekes and Lumley [13]. This equation, along with the continuity equation, describes the outer flow exactly in the limit as the Reynolds number approaches to infinity. The Reynolds normal stresses gradients, $\partial/\partial x[\langle v^2\rangle-\langle u^2\rangle]$ are of the second order compared to the other terms and are usually neglected. However, they will be retained in the present similarity analysis because in flows approaching separation, the contribution of the Reynolds normal stresses gradients is about 30%. (Simpson et al. [14–16], Alving and Fernholz [17], Elsberry et al. [18]). Notice that Eq. (4) does not take into account the case of the large surface curvature where the free stream pressure and the static pressure on the wall are not necessarily the same. On the flat surface, $\partial p/\partial y$ is of the order of δ while on the curvature surface, $\partial p/\partial y$ is of the order of one, Goldstein [19].

2.1 Similarity Solutions. In order to determine the scales of the mean flow and the turbulent quantities, similarity solution forms shown below are sought. The basic assumption is that it is possible to express any dependent variable, in this case the outer deficit velocity, $U-U_\infty$, the outer Reynolds shear stress, $\langle uv\rangle$, and outer Reynolds normal stresses, $\langle u^2\rangle$, $\langle v^2\rangle$ as a product of two functions, i.e.,

$$U-U_\infty=U_{so}(x)f_{op}(\overline{y},\delta^+;\Lambda;*), \tag{5}$$

$$-\langle uv\rangle=R_{so}(x)r_{op}(\overline{y},\delta^+;\Lambda;*), \tag{6}$$

$$\langle u^2\rangle=R_{sou}(x)r_{opu}(\overline{y},\delta^+;\Lambda;*), \tag{7}$$

$$\langle v^2\rangle=R_{sov}(x)r_{opv}(\overline{y},\delta^+;\Lambda;*), \tag{8}$$

where U_{so} and R_{so} are the outer velocity scale and the outer Reynolds shear stress scale, respectively, which depend on x only; R_{sou} and R_{sov} are the Reynolds normal stresses scales corresponding to the $\langle u^2\rangle$ and $\langle v^2\rangle$ components, and depend only on x as well. Note that the outer velocity scale, U_{so}, the outer Reynolds shear stress scale, R_{so}, and the outer Reynolds normal stresses scales, R_{sou} and R_{sov} *must* be determined from the boundary layer equations. The arguments inside the similarity functions (f_{op}, r_{op}, r_{opu}, and r_{opv}) represent the outer similarity coordinate, $\overline{y}=y/\delta_{99}$, the Reynolds number dependence, $\delta^+=\delta u_*/\nu$, the pressure parameter, Λ, and any possible dependence on the upstream conditions,*, respectively.

2.2 Asymptotic Invariance Principle: AIP. This principle means that in the limit as $\mathrm{Re}\rightarrow\infty$ the boundary layer equations become independent of the Reynolds number; therefore, any function or scaling must also be independent of δ^+ as well. Thus, in this limit Eqs. (5) and (6) must also become independent of the local Reynolds number, i.e.,

$$f_{op}(\overline{y},\delta^+;\Lambda;*)\rightarrow f_{op\infty}(\overline{y},\Lambda,*), \tag{9}$$

$$r_{op}(\overline{y},\delta^+;\Lambda;*)\rightarrow r_{op\infty}(\overline{y},\Lambda,*), \tag{10}$$

$$r_{opu}(\overline{y},\delta^+;\Lambda;*)\rightarrow r_{opu\infty}(\overline{y},\Lambda,*), \tag{11}$$

$$r_{opv}(\overline{y},\delta^+;\Lambda;*)\rightarrow r_{opv\infty}(\overline{y},\Lambda,*), \tag{12}$$

as $\delta^+\rightarrow\infty$. The subscript $_\infty$ is used to distinguish these infinite Reynolds number solutions from the finite Reynolds number profiles used in Eqs. (5)–(8).

2.3 Transformed Equations. Using the asymptotic functions of Eqs. (9)–(12), it is possible to get a new outer scale for velocity deficit profiles and Reynolds stresses profiles, respectively. Substituting Eqs. (9)–(12) into Eq. (4) and clearing terms yield:

$$\left[\frac{\delta}{U_{so}}\frac{dU_\infty}{dx}+\left(\frac{U_\infty}{U_{so}}\right)\frac{\delta}{U_{so}}\frac{dU_{so}}{dx}\right]f_{op\infty}+\left[\frac{\delta}{U_{so}}\frac{dU_{so}}{dx}\right]f_{op\infty}^2-\left[\frac{U_\infty}{U_{so}}\frac{d\delta}{dx}+\frac{\delta}{U_{so}}\frac{dU_\infty}{dx}\right]\overline{y}f'_{op\infty}-\left[\frac{d\delta}{dx}+\frac{\delta}{U_{so}}\frac{dU_{so}}{dx}\right]f'_{op\infty}\int_0^{\overline{y}}f_{op\infty}(\tilde{y})d\tilde{y}$$
$$=\left[\frac{R_{so}}{U_{so}^2}\right]r'_{op\infty}-\left[\frac{R_{sov}}{U_{so}^2}\frac{d\delta}{dx}\right]r'_{opv\infty}+\left[\frac{R_{sou}}{U_{so}^2}\frac{d\delta}{dx}\right]r'_{opu\infty}, \tag{13}$$

where the term involving $-dP_\infty/dx$ has been cancelled by the $\rho U_\infty dU_\infty/dx$ term from Euler's equation for the external flow, and the V component is obtained by the integration of the continuity equation.

2.4 Equilibrium Similarity Conditions. For the particular type of "equilibrium" similarity solutions suggested by George [20], all the terms in the governing equations must maintain the same relative balance as the flow develops. These *equilibrium similarity* solutions exist only if all the square bracketed terms have the same x dependence and are independent of the similarity coordinate, $\overline{y}$. Thus, the bracketed terms must remain proportional to each other as the flow develops, i.e.,

$$\frac{\delta}{U_{so}}\frac{dU_{so}}{dx}\sim\frac{\delta}{U_{so}}\frac{dU_\infty}{dx}\sim\left(\frac{U_\infty}{U_{so}}\right)\frac{\delta}{U_{so}}\frac{dU_{so}}{dx}\sim\frac{d\delta}{dx}\sim\left(\frac{U_\infty}{U_{so}}\right)\frac{d\delta}{dx}$$
$$\sim\frac{R_{so}}{U_{so}^2}\sim\frac{R_{sov}}{U_{so}^2}\frac{d\delta}{dx}\sim\frac{R_{sou}}{U_{so}^2}\frac{d\delta}{dx}, \tag{14}$$

where "$\sim$" means "has the same x dependence as." It is clear that full similarity of the "equilibrium-type" is possible only if,

$$U_{so}\sim U_\infty, \tag{15}$$

$$R_{so}\sim U_{so}^2\frac{d\delta}{dx}\sim U_\infty^2\frac{d\delta}{dx}, \tag{16}$$

and

$$R_{sou}\sim R_{sov}\sim U_{so}^2\sim U_\infty^2. \tag{17}$$

Thus, the outer equations do admit to full similarity solutions in the limit of infinite Reynolds number, *and these solutions determine outer scales*. No other choice of scales can produce profiles (of the assumed form), which are asymptotically independent of the Reynolds number, at least unless they reduce to these scales in the limit, George and Castillo [21].

2.5 Pressure Gradient Parameter. Besides the similarity conditions for the mean velocity and Reynolds stresses, other constraint for the pressure gradient can be obtained as well from the analysis such as,

$$\frac{d\delta}{dx} \sim \frac{\delta}{U_\infty}\frac{dU_\infty}{dx} \sim \frac{\delta}{\rho U_\infty^2}\frac{dP_\infty}{dx}. \tag{18}$$

Note, that the pressure gradient controls the growth rate of the boundary layer. A surprising consequence of this condition is that it is satisfied by a power law relation between the free stream velocity and the boundary layer thickness, i.e.,

$$\delta \sim U_\infty^n, \tag{19}$$

where n can, to this point at least, be any nonzero constant. This is the familiar Falker–Skan solutions of laminar boundary layers with pressure gradient discussed by Batchelor [22], but with δ as the variable instead of x. The pressure gradient parameter Λ can be defined as,

$$\Lambda \equiv \frac{\delta}{\rho U_\infty^2 d\delta/dx}\frac{dP_\infty}{dx} = \text{constant} \tag{20}$$

or equivalently

$$\Lambda \equiv -\frac{\delta}{U_\infty d\delta/dx}\frac{dU_\infty}{dx} = \text{constant}. \tag{21}$$

Because equilibrium flows require Λ=constant for similarity, Eq. (21) can be integrated (for nonzero values of Λ) to obtain

$$\delta \sim U_\infty^{-1/\Lambda}. \tag{22}$$

Thus, not only is there a power law relation between the boundary layer thickness and the imposed *free stream* velocity, but the exponent is determined uniquely by the pressure gradient parameter; i.e.,

$$n = -\frac{1}{\Lambda}. \tag{23}$$

Therefore, an "equilibrium" boundary layer *in the present approach* is one where Λ=constant and $\delta \sim U_\infty^{-1/\Lambda}$.

2.6 Relations Between the Length Scales and Λ. The goal in this section is to show that the pressure gradient parameter, Λ, can be expressed in terms of the displacement thickness, δ_*, or the momentum thickness, θ. Using the definitions of the momentum thickness, θ, and the displacement thickness, δ_*, it is possible to show that $\theta \sim \delta \sim \delta_*$ according to Castillo [23]. Therefore, the pressure parameter in terms of the momentum thickness is given as,

$$\Lambda_\theta \equiv \frac{\theta}{\rho U_\infty^2 d\theta/dx}\frac{dP_\infty}{dx} = -\frac{\theta}{U_\infty d\theta/dx}\frac{dU_\infty}{dx} = \text{constant}, \tag{24}$$

and in term of the displacement thickness as,

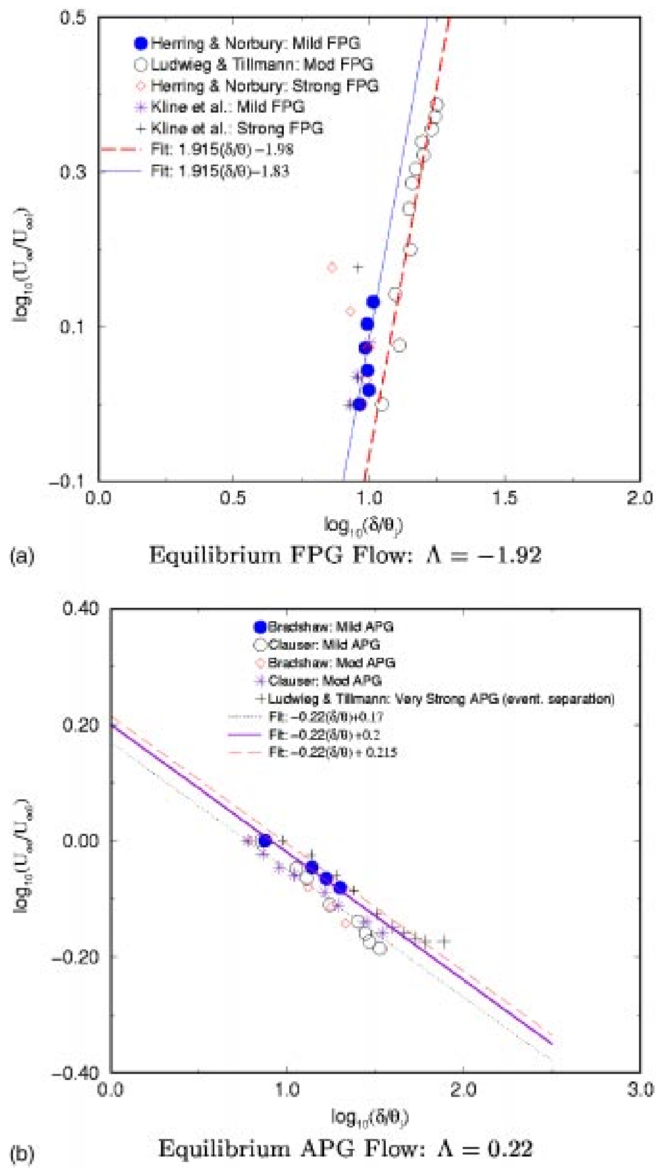

Fig. 1 Plots of log(U_∞) vs log(δ_{99}) for FPG and APG data. The plot is normalized with $U_{\infty i}$ and θ_i for the first measured location Castillo and George [2].

$$\Lambda_{\delta *} \equiv \frac{\delta_*}{\rho U_\infty^2 d\delta_*/dx}\frac{dP_\infty}{dx} = -\frac{\delta_*}{U_\infty d\delta_*/dx}\frac{dU_\infty}{dx} = \text{constant}. \tag{25}$$

Since $\theta \sim \delta \sim \delta_*$ exists at least in the limit of Re→∞, it is easily to obtain

$$\Lambda_\theta \sim \Lambda_{\delta_*} \sim \Lambda. \tag{26}$$

Thus, asymptotically at least, the following relationship

$$U_\infty \sim \delta^{-\Lambda} \sim \delta_*^{-\Lambda_{\delta *}} \sim \theta^{-\Lambda_\theta} \tag{27}$$

exists.

But what is the relation between these pressure parameters at the finite Reynolds number of experiments? Castillo [24] and Castillo et al. [25] were able to show from experiments that all velocity profiles for nonseparating adverse pressure gradient boundary layers could be collapsed onto a single curve using the scaling proposed by Zagarola/Smits [26], $U_\infty \delta_*/\delta$. They also

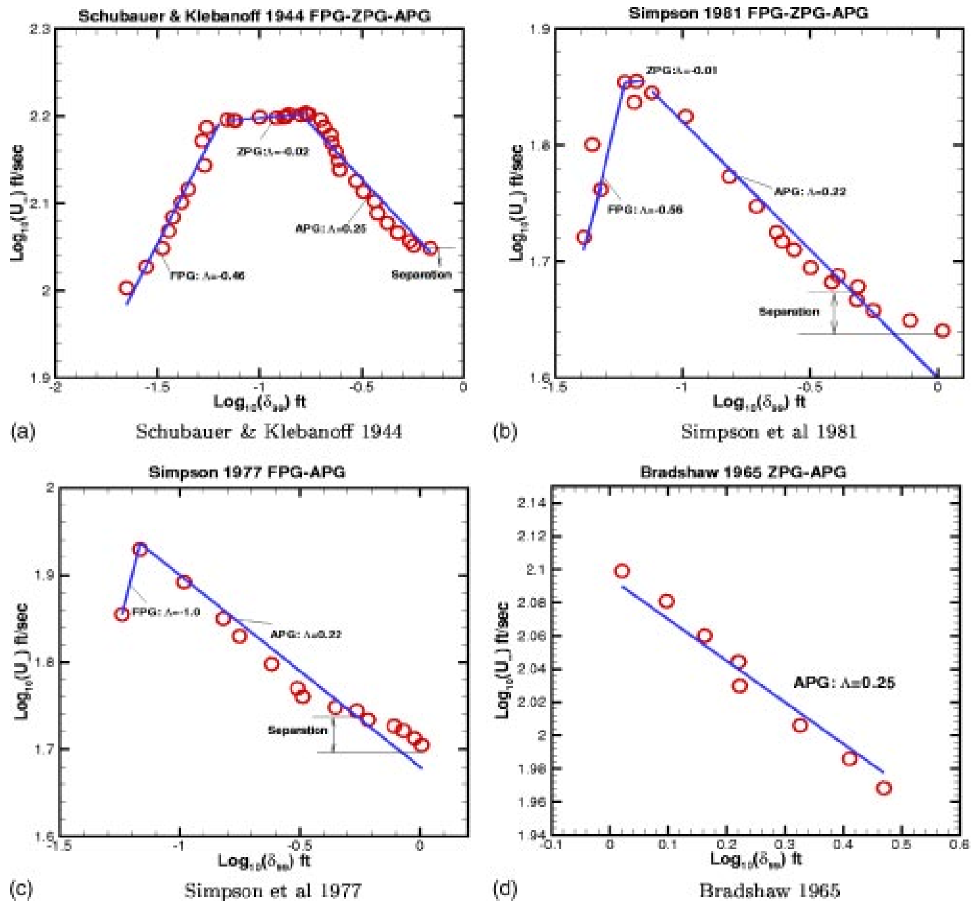

Fig. 2 Nonequilibrium boundary layers: Plots of log(U_∞) vs log(δ_{99})

showed that the same profiles collapsed to a single curve using U_∞ only if the upstream conditions were fixed as shown by Walker and Castillo [27] and Castillo and Walker [28]. Thus all of the variation among different sets of data could be attributed to the upstream conditions. They showed that the ratio δ_*/δ was approximately constant for fixed upstream conditions. Wosnik [29] argued that for ZPG flow, a necessary consequence of the observed success of the Zagarola/Smits scaling was that the ratio $\tilde{\delta}_*/\delta$ be exactly a constant, but the constant differed for different upstream conditions. The length scale $\tilde{\delta}_*$ was calculated like the displacement thickness, but only using data *outside* $y/\delta > 0.1$.

Clearly, an equilibrium flow exists only if the data show a linear relation between the logarithmic length scales and the logarithmic free stream velocity. Also, the slope should correspond to the value of each pressure parameter (i.e., Λ, Λ_θ, and Λ_{δ_*}). Previous investigation by Castillo and George [2] suggested that the pressure parameter is given by $\Lambda \cong 0.22$ for APG equilibrium flow and $\Lambda \cong -1.92$ for FPG equilibrium flow as shown in Fig. 1. Figure 1(a) shows various FPG experimental data of $\log(U_\infty/U_{\infty i})$ versus $\log(\delta/\theta_i)$. In order to compare the results from different experiments, the free stream velocity, U_∞, and the boundary layer thickness, δ, were normalized by $U_{\infty i}$ and θ_i, where the subscript i means the first downstream location. Since all the data (at least away from the entrance and exit) have approximately the same slope, it is clear that $\Lambda \cong -1.92$ is a suitable description of these data even though the strength of the pressure gradient varies from mild, moderate to strong FPG. A similar behavior occurs for APG flows with different strengths of pressure gradient shown in Fig. 1(b). Clearly, $\Lambda \cong 0.22$ describes properly most of equilibrium APG flows. But, can the APG region of a nonequilibrium flow be described by the same value of the pressure parameter, $\Lambda \cong 0.22$? Also, what are the values of the pressure parameter for the FPG region or ZPG region of a nonequilibrium flow?

3 Nonequilibrium Flows

Figures 2 and 3 show some cases of nonequilibrium turbulent boundary layers. Figure 2 displays a nonlinear relationship between $\log(U_\infty)$ vs $\log(\delta)$ corresponding to each experiment described below. Figure 3 shows the same experimental data using the momentum thickness, θ, as the length scale. Consequently, the pressure parameter Λ and Λ_θ are obtained. Notice that θ is an integral value over the whole profile, whereas δ is just a local value at a certain position (i.e., δ_{95} or δ_{99}). Therefore, there are less errors associated with the calculation of θ than δ_{99} or δ_{95}. Notice that Fig. 3 shows a better linear relation between $\log(U_\infty)$ vs $\log(\theta)$ than $\log(U_\infty)$ vs $\log(\delta)$ in Fig. 2.

For the nonequilibrium data from Schubauer and Klebanoff [30] ($1420 < Re_\theta < 76\,700$), and Simpson et al. [15] ($1380 < Re_\theta < 18\,700$), the external PG changes from FPG to ZPG and then from ZPG to APG with eventual separation. It is obvious that these flows are not in equilibrium since globally the pressure parameter is not a constant. However, they remain in equilibrium locally. Another interesting fact is that there are three distinctive regions: one for FPG with $\Lambda_\theta = -0.44$ (for Schubauer and Klebanoff [30]), $\Lambda_\theta = -0.8$ (for Simpson et al. [15]); one for ZPG with $\Lambda_\theta = -0.03$ (for Schubauer and Klebanoff [30]), $\Lambda_\theta = 0$ (for Simpson et al. [15]); and one for the APG region with $\Lambda_\theta = 0.22$ for both cases.

A similar behavior occurs for the experimental data from Simpson et al. [31] ($2240 < Re_\theta < 38\,000$) as shown in Figs. 2(c) and

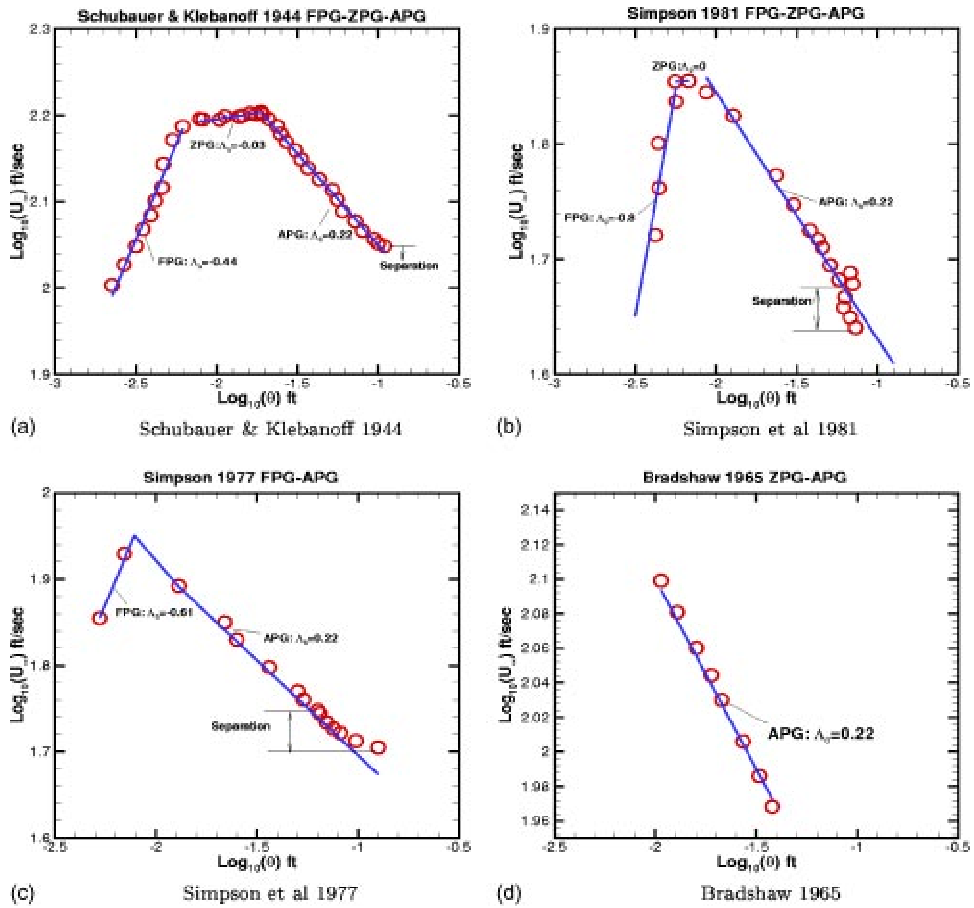

Fig. 3 Nonequilibrium boundary layers: Plots of log(U_∞) vs log(θ)

3(c). For this experimental data, there are two distinctive regions: one for the FPG and one for the APG region. Each region is locally in equilibrium, and is characterized by a constant pressure parameter $\Lambda_\theta = -0.61$ for the FPG region and $\Lambda_\theta = 0.22$ for the APG region, respectively. Meanwhile, for the measurements of relax flow from Bradshaw [12] ($8593 < \mathrm{Re}_\theta < 22\,582$) shown in Figs. 2(d) and 3(d), the flow still remains in equilibrium with $\Lambda_\theta = 0.22$ even when it undergoes a sudden change in pressure gradient from ZPG to APG.

In addition, notice that for the experimental data from Schubauer and Klebanoff [30] and Simpson et al. [15,31], the flow eventually separates and it is indicated in Figs. 2 and 3. Moreover, the experimental data by Simpson et al. [15,31] show a long range of separation.

Clearly, $\Lambda_\theta \cong 0.22$ exists for the APG region of nonequilibrium flows, which is same as the pressure parameter Λ for equilibrium boundary layers as reported by Castillo and George [2]. In addition, Castillo et al. [11] showed that the pressure parameter Λ_θ for separated flows was close to 0.21. Table 1 summarized all results from the equilibrium flows of Castillo and George [2] and Wang [32], the results from separated flows in the analysis of Castillo et al. [11], and the results from the present investigation.

4 Zagarola/Smits Scaling Using Similarity Analysis

Most recently, Castillo and Walker [28] showed that using the Zagarola/Smits scaling [26] for all APG flows, velocity deficit profiles collapse into a single curve, which is an indication that all APG flows (at least equilibrium flows) could be characterized by a single profile. Since the pressure parameter is a constant with $\Lambda_\theta \cong 0.21$ or 0.22 for all equilibrium and nonequilibrium boundary layers with APG, it means that it is possible to represent APG flows for equilibrium boundary layers with one profile and for nonequilibrium flows with the similar approaches.

Table 1 Pressure parameter for equilibrium and nonequilibrium flows

	Experiments	APG
Equilibrium flows Λ_θ: Castillo and George [2], Wang [32]	Bradshaw Mild and Mod APG, Clauser Mild and Mod APG, Ludwig and Tillman strong APG and Mod APG; Skåre and Krogstad APG, Marusic APG, and Elsberry et al. Strong APG.	0.21 ± 0.04
Separation flows Λ_θ: Castillo, Wang and George [11]	Newman strong APG, Alving and Fernholz, Ludwig and Tillman, Simpson et al. 1977, Simpson et al. 1981	0.21 ± 0.01
Nonequilibrium flows Λ_θ:	Schubauer and Klebanoff FPG-ZPG-APG 1944, Bradshaw ZPG-APG 1965, Simpson et al. FPG-APG 1977, Simpson et al. FPG-ZPG-APG 1981	0.22

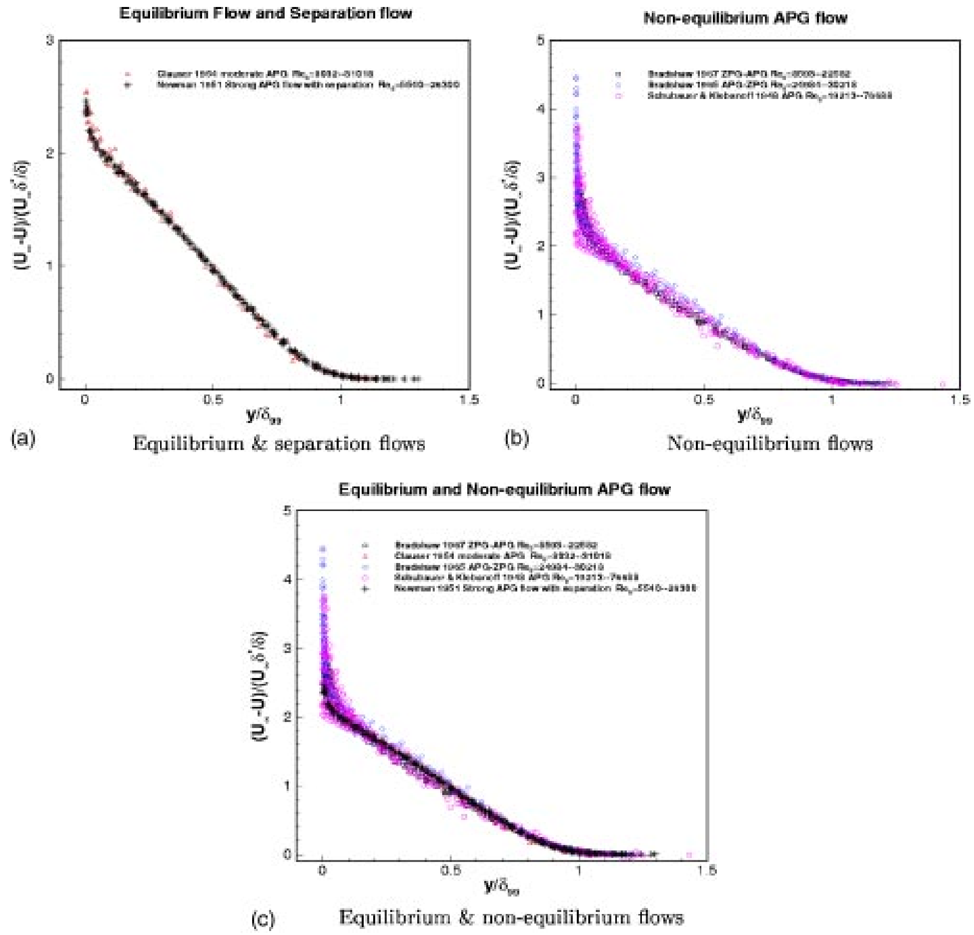

Fig. 4 APG velocity profiles using Zagarola/Smits scaling: nonequilibrium flows and equilibrium flows

Using the similarity ideas outlined in the previous sections, the empirical velocity scaling of Zagarola/Smits [26], $U_{so} = U_\infty(\delta_*/\delta)$, will be derived in this section. It is assumed that the function f_{op} can be expressed as a product of two functions, i.e.,

$$f_{op}(\overline{y},\delta^+;\Lambda;*) = G(\delta^+;*)F_{op\infty}(\overline{y};\Lambda). \tag{28}$$

The first term $G(\delta^+;*)$ contains the dependence on the Reynolds number, δ^+, and the upstream conditions,*, while the second term $F_{op\infty}(\overline{y};\Lambda)$ contains the normalized dependence on the distance from the wall, $\overline{y}$, and the pressure parameter, Λ. This profile, $F_{op\infty}$, represents the asymptotic velocity profile in the limit as $\mathrm{Re}\rightarrow\infty$. It is this profile that must reduce to a similarity solution of the RANS equations as required by the asymptotic invariance principle. Hence, this asymptotic profile must be independent of Reynolds number, but its shape may be different for ZPG, FPG, and APG turbulent flows depending on the values of the pressure parameter, Λ. Note, that a similar decomposition of the profile was used by Wosnik and George [33] for ZPG boundary layers.

For the incompressible flow, the displacement thickness is given by

$$U_\infty\delta_* = \int_0^\infty (U_\infty - U)dy. \tag{29}$$

The function, $G(\delta^+,*)$, can be determined by substituting Eq. (28) into the definition for the displacement thickness Eq. (29):

$$[\delta_*]\approx[\delta G]\int_0^\infty F_{op\infty}(\overline{y},\Lambda)d\overline{y}, \tag{30}$$

where a small contribution from the inner layer has been neglected. It is easy to show that Eq. (30) is exact in the limit of the infinite Reynolds number. Now, since Eq. (30) is in similarity variables, the integral part depend on Λ at most, which itself must be independent of x. Therefore, δ and δ_* must have the same x dependence. It follows immediately that,

$$G\propto(\delta_*/\delta). \tag{31}$$

The function G can be combined with Eqs. (4) and (28) to yield the outer velocity scale of Zagarola/Smits, $U_{so}=U_\infty(\delta_*/\delta)$. Note the fact that the Zagarola/Smits scaling contains the Reynolds number dependence term, δ_*/δ, which means that the boundary layer is indeed Reynolds number dependent, exactly as argued by Castillo and George [2] and George and Castillo [21].

Castillo and Walker [28] showed that $\delta_*/\delta\rightarrow$constant in the limit of the infinite *local* Reynolds number, but argued that the constant might depend on the upstream conditions. This result obeys the Asymptotic Invariance Principle, which requires that any properly scaled similarity function must be asymptotically independent of Reynolds number. Thus, in the limit as $\delta^+\rightarrow\infty$, $G\rightarrow G_\infty(*)$ only. Therefore, if the proposed separation of f_{op} is valid, all of the effects of upstream conditions should be removed by the Zagarola/Smits scaling. Or conversely, if the Zagarola/

Smits scaling proves successful, then the separation of solution must be at least approximately valid in the limit as $\delta^+ \to \infty$.

It is important to note that since $\delta_*/\delta \to$constant as $\delta^+ \to \infty$, the Zagarola/Smits scaling, $U_\infty(\delta_*/\delta)$, reduces to the GC scaling, U_∞, in the same limit. Thus, both the U_∞ and $U_\infty \delta_*/\delta$ scalings are consistent with the equilibrium similarity analysis. The latter, of course, also removes the upstream and local Reynolds number effects, if the hypothesis of Eq. (28) is correct. This can be contrasted with the analysis of Clauser [1] which requires that $U_\infty \delta_*/\delta \sim u_*$. Obviously, if this classical result is correct, there should be no difference between the ZS-scaled profiles and those using u_*, contrary to the finding of Zagarola and Smits [26].

Figure 4 shows the velocity profiles normalized by the Zagarola/Smits scaling for the APG experimental data of Bradshaw [34] initially at ZPG developing into a sudden moderate APG, the Bradshaw [12] data for relaxed flow, the Clauser [1] data for moderate APG, the Newman [35] experimental data with eventual separation and finally the Schubauer and Klebanoff [30] data for nonequilibrium flow. Notice that the experimental data from Clauser [1] and Newman [35] are in equilibrium. However, the other three measurements are nonequilibrium flows because the pressure parameter is not a constant. Also, for the measurement by Schubauer and Klebanoff [30], the flow eventually separates. In spite of all the differences, the APG velocity profiles collapse into nearly one single curve. Figure 4(a) shows some of the profiles from equilibrium boundary layers as given by Castillo and George [2]. Clearly, there is a single velocity profile for the equilibrium APG flow while normalized by the Zagarola/Smits scaling. The nonequilibrium deficit profiles are shown in Fig. 4(b). Notice that there is nearly a single profile for these nonequilibrium flows as described by the single pressure parameter Λ_θ. Figure 4(c) includes the equilibrium and nonequilibrium APG flows and the profiles follow nearly only one curve too.

5 Summary and Conclusions

Using similarity analysis for nonequilibrium flows, the main results of the present investigation can be summarized as:

1. Nonequilibrium boundary layers, defined as $\Lambda_\theta \neq$constant, remain in equilibrium, but only locally with a pressure parameter, Λ_θ=constant, for each region.

2. Each local region is characterized by a constant pressure parameter. For the FPG region of a nonequilibrium flow, the pressure parameter varies from -0.44 up to -0.8. For the ZPG region of a nonequilibrium flow, the pressure parameter is nearly zero. The APG region of the current nonequilibrium flow has the value of about $\Lambda_\theta \cong 0.22$, which is the same as the pressure parameter for the equilibrium flow in terms of Λ.

3. It has been found that nearly a single velocity profile exists for all APG flows including equilibrium and nonequilibrium flows when scaled by the Zagarola/Smits scaling.

In conclusion, flows that are exposed to sudden external changes in pressure gradient (PG) still remain in a local equilibrium. Moreover, the similarity theory proves to be a powerful tool to understand PG flows and their tendency to remain in equilibrium state.

Acknowledgment

The authors are very grateful to the reviewers for their insightful comments and suggestions which result in an improved paper.

Nomenclature

R_{so} = outer Reynolds stress scale for $\langle uv \rangle$
R_{sou} = outer Reynolds stress scale for $\langle u^2 \rangle$
R_{sov} = outer Reynolds stress scale for $\langle v^2 \rangle$
U_{so} = outer velocity scale
U_∞ = free stream velocity
$U_\infty - U$ = mean velocity deficit
$U_\infty \delta_*/\delta$ = Zagarola/Smits scaling
u_* = friction velocity, $u_* = \sqrt{\tau_w/\rho}$
δ = boundary layer thickness, e.g., δ_{99}
δ_* = displacement thickness, $\int_0^\infty (1-U/U_\infty)dy$
δ^+ = local Reynolds number dependence, $\delta u_*/\nu$
Λ = pressure parameter, $(\delta/\rho U_\infty^2 d\delta/dx)(dP_\infty/dx)$
Λ_{δ_*} = pressure parameter, $(\delta_*/\rho U_\infty^2 d\delta_*/dx)(dP_\infty/dx)$
Λ_θ = pressure parameter, $(\theta/\rho U_\infty^2 d\theta/dx)(dP_\infty/dx)$
θ = momentum thickness, $\int_0^\infty (U/U_\infty)(1-U/U_\infty)dy$
$*$ = unknown upstream conditions
PG = pressure gradient
ZPG = zero pressure gradient
FPG = favorable pressure gradient
APG = adverse pressure gradient

References

[1] Clauser, F. H., 1956, ''The Turbulent Boundary Layer,'' Adv. Appl. Mech., **4**, pp. 1–54.
[2] Castillo, L., and George, W. K., 2001, ''Similarity Analysis for Turbulent Boundary Layer With Pressure Gradient: Outer Flow,'' AIAA J., **39**, pp. 41–47.
[3] Bradshaw, P., 1967, ''The Turbulent Structure of Equilibrium Boundary Layers,'' J. Fluid Mech., **29**, pp. 624–645.
[4] Townsend, A. A., 1956, The Structure of Turbulent Shear Flow, Cambridge University Press, London.
[5] Rotta, J. C., 1962, ''Turbulent Boundary Layers in Incompressible Flow,'' *Progr. Aeronautical Sci.*, Vol. 2., Pergamon, New York.
[6] Townsend, A. A., 1976, *The Structure of Turbulent Shear Flow*, 2nd ed., Cambridge, London.
[7] East, L. F., and Sawyer, W. G., 1979, ''An Investigation of the Equilibrium Turbulent Boundary Layers,'' Turbulent Boundary Layers: Experiment Theory and Modelling, AGARD, CP-271, 6.1–6.19.
[8] Skåre, P. E., and Krogstad, P., 1994, ''A Turbulent Equilibrium Boundary Layer Near Separation,'' J. Fluid Mech., **272**, pp. 319–348.
[9] Kader, B. A., and Yaglom, A. M., 1977, ''Similarity Treatment of Moving-Equilibrium Turbulent Boundary Layers in Adverse Pressure Gradients,'' J. Fluid Mech., **89**, pp. 305–342.
[10] Coles, D. E., and Hirst, E. A., 1968, Computational of Turbulent Boundary Layers-1968 AFOSR-IFP-Stanford Conference, Vol. II.
[11] Castillo, L., Wang, X., and George, W., 2003, ''Separation Criterion for Turbulent Boundary Layers via Similarity Analysis,'' J. Fluid Eng. **126**, pp. 297–304.
[12] Bradshaw, P., and Ferriss, D., 1965, ''The Response of a Retarded Equilibrium Turbulent Boundary Layer to the Sudden Removal of Pressure Gradient,'' NPL Aero. Rep., 1145.
[13] Tennekes, H., and Lumley, J. L., 1972, *A First Course in Turbulence*, MIT, Cambridge, MA.
[14] Simpson, R. L., 1989, ''Turbulent Boundary-Layer Separation,'' Annu. Rev. Fluid Mech., **21**, pp. 205–234.
[15] Simpson, R. L., and Chew, Y. T., 1981, ''The Structure of a Separating Turbulent Boundary Layer. Part 1. Mean Flow and Reynolds Stresses,'' J. Fluid Mech., **113**, pp. 23–51.
[16] Simpson, R. L., and Chew, Y. T., 1981, ''The Structure of a Separating Turbulent Boundary Layer. Part 2. Higher-Order Turbulence Results,'' J. Fluid Mech., **113**, pp. 53–73.
[17] Alving, A. E., and Fernholz, H. H., 1995, ''Turbulence Measurements Around a Mild Separation Bubble and Down-Stream of Reattachment,'' J. Fluid Mech., **322**, pp. 279–328.
[18] Elsberry, K., Loeffler, J., Zhou, M. D., and Wygnanski, I., 2000, ''An Experimental Study of a Boundary Layer That is Maintained on the Verge of Separation,'' J. Fluid Mech., **423**, pp. 227–262.
[19] Goldstein, S., ''*Modern Developments in Fluids Dynamics*,'' 1965, Dover, New York.
[20] George, W. K., 1995, ''Some New Ideas for Similarity of Turbulent Shear Flows,'' *Turbulence, Heat and Mass Transfer*, edited by K. Hanjalic and J. C. F. Pereira, Begell House, New York.
[21] George, W. K., and Castillo, L., 1997, ''Zero-Pressure-Gradient Turbulent Boundary Layer,'' Appl. Mech. Rev., **50**, pp. 689–729.
[22] Batchelor, G. K., 1966, *An Introduction to Fluid Dynamics*, Cambridge Univeristy Press, London.
[23] Castillo, L., 1997, ''Similarity Analysis of Turbulent Boundary Layers,'' Ph.D. dissertation, SUNY Buffalo, Buffalo, NY.
[24] Castillo, L., 2000, ''Application of Zagarola/Smits Scaling in Turbulent Boundary Layers With Pressure Gradient,'' Advances in Fluids Mechanics 3, Montreal, Canada, May 24–26, 2000, edited by M. Rahman and C. A. Brebbia, pp. 275–288.
[25] Castillo, L., Walker, D. J., and Wosnik, M., 2000, ''The Effect of the Upstream Conditions on the Mean Velocity Deficit of Turbulent Boundary Layers,'' Fluids 2000 Conference and Exhibit paper #AIAA2000–2309. Denver, Colorado, June 19–22.
[26] Zagarola, M. V., and Smits, A. J., 1998, ''Mean-Flow Scaling of Turbulent Pipe Flow,'' J. Fluid Mech., **373**, pp. 33–79.
[27] Walker, D., and Castillo, L., 2002, ''Effect of the Upstream Conditions on

Turbulent Boudnary Layers,'' AIAA J., **40**, pp. 2540–2542.
[28] Castillo, L., and Walker, D., 2002, ''The Effect of the Upstream Conditions on the Outer Flow of Turbulent Boundary Layers,'' AIAA J., **40**, pp. 1292–1299.
[29] Wosnik, M., 2000, ''On Wall-Bounded Turbulent Flows,'' Ph.D. thesis, SUNY Buffalo, Buffalo, NY.
[30] Schubauer, G. B., and Klebanoff, P. S., 1951, ''Investigation of Separation of the Turbulent Boundary Layer,'' NACA Report 1030, NACA Technical Note 2133.
[31] Simpson, R. L., and Strickland, J. H., 1977, ''Features of a Separating Turbulent Boundary Layer in the Vicinity of Separation,'' J. Fluid Mech., **79**, pp. 553–594.
[32] Wang, X., ''Similarity Analysis for Turubulent Boundary Layers Subject to Pressure Gradient and Heat Transfer,'' 2003, Ph.D. dissertation, Rensslaer Polytechnic Institute, Troy, NY.
[33] Wosnik, M., and George, W. K., 2000, ''Reconciling the Zagarola/Smits Scaling With the George/Castillo Theory for the Zero Pressure Gradient Turbulent Boundary Layer,'' 38th AIAA Ann. Atg. Reno, NV, Jan 10–13.
[34] Bradshaw, P., 1967, ''The Response of a Constant-Pressure Turbulent Boundary Layer to the Sudden Application of an Adverse Pressure Gradient,'' NPL Aero. Rept. 1219.
[35] Newman, B. G., 1951, ''Some Contributions to the Study of the Turbulent Boundary Near Separation,'' Austr. Dept. Supply Rep. ACA-53.